Geoid
Journal of Geodesy and Geomatics

Geoid Vol. 19, No. 3, 2024, 508-518

P-ISSN: 1858-2281; E-ISSN: 2442-3998

Predictive Modeling of Terrestrial Water Storage Anomalies in Kalimantan Basins: Bridging the GRACE and GRACE-FO Data Gap with Extreme Gradient Boosting

Rizka Amelia Dwi Safira[1], Ira Mutiara Anjasmara*[1], Joseph L. Awange[2]
[1]Department of Geomatics Engineering, Institut Teknologi Sepuluh Nopember, Surabaya, Indonesia
[2]School of Earth and Planetary Sciences, Spatial Sciences Discipline, Curtin University, Perth, WA, Australia
*Corresponding author: i.anjasmara@ its.ac.id

Received: 24102024; Revised: 16122024; Accepted: 16122024; Published: 16122024

Abstract: Terrestrial water storage (TWS) anomaly has been a robust indicator in predicting and monitoring hydrometeorological hazards and sustainable water resources management to comprehend the water dynamics on Earth. The Gravity Recovery and Climate Experiment (GRACE) satellite identifies this change by heeding the Earth's mass anomalies since 2002. However, due to an 11-month data gap before the operation of GRACE-FO, continuous investigation using GRACE has been challenging. This study employed an extreme gradient boosting (XGBoost) algorithm to reconstruct GRACE TWS anomaly by integrating the hydroclimatic variables from Noah surface models over a span of approximately 20 years, focusing on five Kalimantan basins. The testing set was evaluated using three statistical metrics, resulting in a correlation coefficient (CC) of 0.943, Nash–Sutcliffe efficiency (NSE) of 0.887, and scaled root-mean-square error (RMSE*) of 0.337. This approach effectively addresses the research gap in utilizing the GRACE product in an archipelago state such as Indonesia and offers an efficient method for reconstructing TWS anomalies for various hydrological systems at the local scale.

Keywords : GRACE; GRACE-FO; Terrestrial Water Storage Anomaly; machine learning; water dynamics.

How to cite: Safira, R. A. D., Anjasmara, I. M., Awange, J. L. (2024). Predictive Modeling of Terrestrial Water Storage Anomalies in Kalimantan Basins: Bridging the GRACE and GRACE-FO Data Gap with Extreme Gradient Boosting. *Geoid, 19*(3), 508 - 518

Introduction

Terrestrial water storage (TWS) encompasses water accumulated on and below the Earth's surface, including soil moisture, root zone soil moisture, groundwater, snow, ice, vegetation storage, rivers, and lakes, tracking water cycle changes due to natural and human factors (Awange et al., 2008; Girotto & Rodell, 2019). At the same time, global water resources are unevenly distributed, leading to challenges of availability and scarcity exacerbated by human mismanagement (Senent-Aparicio et al., 2018). As one of the world's largest archipelagos, Indonesia exhibits diverse climatological patterns, rainfall variability, topography, land cover, basin sizes, population densities, and water needs for irrigation, domestic use, households, government, and industries (Mediawan et al., 2021). Evaluating water resources is crucial for effective catchment management (Wurbs, 2005), enabling proactive risk mitigation and sustainable water resource management to understand Indonesia's water dynamics moving forward.

The GRACE (Gravity Recovery and Climate Experiment) satellite has been pivotal in providing quasi-global Terrestrial Water Storage Anomaly (TWSA) data since April 2002 (Xiong et al., 2021). GRACE detects changes in Earth's water mass and distribution, enabling the identification of hydrometeorological hazards, such as flood and hydrological drought, as anomalies (Cui, 2019; Jiang et al., 2023; Rateb et al., 2024; Tapley et al., 2019; Zhu et al., 2023). A gap in data occurred when GRACE ceased operation in October 2017, before the launch of its successor, GRACE-FO (Follow-on), in May 2018, causing a nearly one-year discontinuity.

This led to biases and uncertainties in hydrological models assimilated with GRACE TWSA data (Mo et al., 2022).

Previous studies have employed machine learning and deep learning algorithms to gap-fill the GRACE data. Traditional methods such as interpolation and sensor dependency are ineffective for long-term gaps or improving resolution. Interpolation fails to present new information in reconstructions due to its reliance on existing data, leading to potential accuracy limitations. Similarly, sensor-dependent methods using Swarm satellites cannot replicate high-frequency TWSA signals (Lai et al., 2022). Jiang et al. (2023) and Kumar et al. (2022) used a Multilayer Perceptron-Artificial Neural Network (MLP-ANN) to reconstruct GRACE TWSA for the Yarlung Tsangpo Brahmaputra River Basin and Telangana State in India, achieving high CC (0.96) and low RMSE (1.99 cm) using precipitation, temperature, and GLDAS (Global Land Data Assimilation System) hydrological models as predictors. (Sun et al., 2020) filled GRACE TWSA data gaps with a Deep Neural Network (DNN) for 60 global basins, including the Barito River Basin in Kalimantan, achieving varied results (CC = 0.88-0.95; RMSE = 4.5-10.6 cm).

Based on the outlined background, this study aims to reconstruct hydrological patterns from GRACE/GRACE-FO data by integrating hydroclimatic model data and machine learning methods. This approach remains relatively underexplored, especially in Indonesia, a vast archipelagic nation. Focusing on Kalimantan Island, the largest island of Indonesia with several extensive surface water bodies and basins as well as the future site of Indonesia's new capital, this study seeks to fill the gap and understand the anomaly in Terrestrial Water Storage (TWS) from 2003 to 2022.

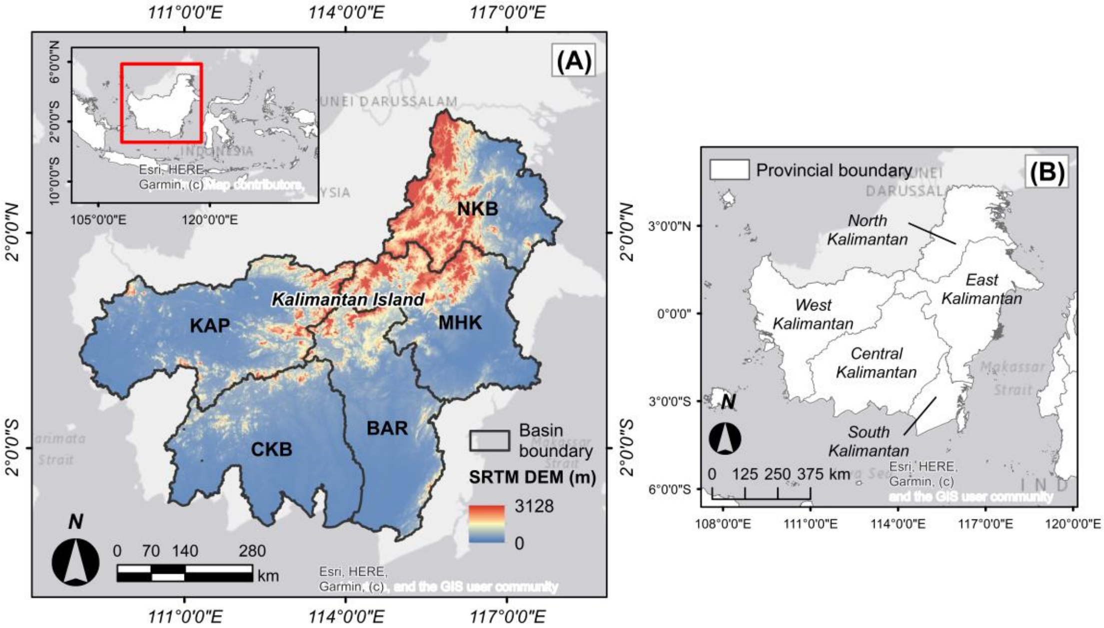

Figure 1. Study region. (A) Kalimantan basins: NKB (Northern Kalimantan), MHK (Mahakam), BAR (Barito), CKB (Central Kalimantan), and KAP (Kapuas) basins, blue to red colors indicate the surface elevation based on SRTM Digital Elevation Data Version 4 (https://srtm.csi.cgiar.org); (B) Provincial administration boundary.

Data and Method

Five basins, comprising Northern Kalimantan (NKB) (67,871.51 km^2), Mahakam (MHK) (77,423 km^2), Barito (BAR) (62,355.59 km^2), Central Kalimantan (CKB) (80,478.66 km^2), and Kapuas (KAP) (100,284.04 km^2), basins, were designated as the study region in this research (Figure 1). NKB and CKB were defined as larger basins by merging several smaller basins. NKB consists of Sesayap, Kayan, Belayau, and Berau basins; while CKB includes Kahayan, Sebangau, Katingan, Mentaya, Seruyan, Kotawaringin, and Jelai basins. The varying rainfall patterns and irrigation coverage areas influence the variability of TWS change over the study region. As a primary factor in water budgeting, rainfall plays a crucial role in the global water cycle and is a key driver of TWS changes (Humphrey et al., 2023). Additionally, the extent of irrigated areas affects the volume of water used in agricultural systems (Tirtalistyani et al., 2022). According to BMKG (2021), monsoonal precipitation patterns are observed in the southern regions of West, Central, and East Kalimantan. North Kalimantan and the northern parts of West, Central, and East Kalimantan exhibit equatorial patterns. In 2017, the irrigated areas in West, Central, South, East, and North Kalimantan were significantly smaller compared to densely populated islands like Java, measuring 91,561 ha, 13,850 ha, 47,203 ha, 11,875 ha, and 3,978 ha, respectively (Pusat Data dan Sistem Informasi Pertanian, 2020).

1. Data

This research incorporates GRACE/GRACE-FO terrestrial water storage anomaly (TWSA) data and GLDAS components. This research used GRACE/GRACE-FO Mascon Ocean, Ice, and Hydrology Equivalent Water Height (EWH) Coastal Resolution Improvement (CRI) Filtered Release 06.1 v.03 (Wiese et al., 2023) during 2003-2022. This dataset is monthly gridded data in 0.5° spatial resolution with its native resolution of 3°× 3° equal area and produced by Jet Propulsion Laboratory (JPL). This study employed a simple linear interpolation method to fill the 21 months of short-term monthly data gaps (1-2 months) from 2003 to 2022, as applied by (Alshehri & Mohamed, 2023; Wang et al., 2020). This interpolation process results in a GRACE TWSA with 11 consecutive months of data gaps. Subsequently, this study utilized Noah GLDAS V2.1 because of its identical reliability with GRACE products (Beaudoing & Rodell, 2020; Kumar et al., 2022). Noah GLDAS is monthly gridded data with 0.25° spatial resolution. Table 1 summarizes the ten parameters of Noah GLDAS employed in this study as the input variables in TWSA prediction.

Table 1. Noah GLDAS data as input variables in TWSA prediction.

Input variables	**Noah GLDAS parameters/unit**	**Parameter description**
Precipitation (P)	Rainf_tavg/kg m^{-2} s^{-1}	Rain precipitation rate
Evapotranspiration (ET)	Evap_tavg/kg m^{-2} s^{-1}	Evapotranspiration
Runoff (Q)	Qs_acc/kg m^{-2}	Storm surface runoff
	Qsb_acc/kg m^{-2}	Baseflow-groundwater runoff
Soil moisture storage anomaly (SMSA)	SoilMoi0_10cm_inst/kg m^{-2}	Soil moisture (0-10 cm)
	SoilMoi10_40cm_inst/kg m^{-2}	Soil moisture (10-40 cm)
	SoilMoi40_100cm_inst/kg m^{-2}	Soil moisture (40-100 cm)
	SoilMoi100_200cm_inst/kg m^{-2}	Soil moisture (100-200 cm)
Plant canopy storage anomaly (PCSA)	CanopInt_inst/kg m^{-2}	Plant canopy surface water
Temperature (T)	Tair_f_inst/K	Air temperature
[a] Noah-derived TWSA (N)	-	-

2. Methods

Three primary stages of the data processing are illustrated as a flowchart in Figure 2. First, GRACE/GRACE-FO data with a 0.5° resolution, including gaps over eleven months, serves as the dependent variable. The independent variables are initially at a 0.25° resolution and resampled to match the 0.5° resolution of the GRACE/GRACE-FO data. In predicting hydrometeorological phenomena, analyzing the time-lag effect of hydrological variables on TWS requires considering periods ranging from months to years (Barker et al., 2016; Melo & Wendland, 2016). This effect highlights how hydrological variables propagate through the terrestrial hydrological cycle (Yang, 2017). This study builds on previous research by employing a three-month lag to explain TWS anomalies (Gyawali et al., 2022; Wang et al., 2023), linking hydrological variable x from months i, i-1, i-2, to i-3 with TWSA in month i.

Second, data is split randomly into training and testing (80/20) sets. The training set is decomposed into trend and detrend components, with detrend training used to predict TWSA values. Testing evaluates the training results, focusing on detrend data, as predictors do not indicate TWS trends, and the one-year data gap has minimal impact. Trends are reintroduced post-modeling using XGBoost (Lai et al., 2022). XGBoost is a tree-boosting algorithm that utilizes an exceptional strategy for model optimization using the gradient method. XGBoost offers scalability, enabling it to handle large and intricate datasets effectively, delivering performance gains up to ten times compared to other tree-boosting algorithms (Chen & Guestrin, 2016). The trees built in XGBoost are interdependent (Ali et al., 2022). In hydrology fields, regression applications using the XGBoost algorithm are applied to reconstruct signals on time series (Ali et al., 2023; Sahour et al., 2020; Zhang et al., 2021). The XGBoost modeling can be set using the *'xgboost'* package in R language (Chen et al., 2020). We determined the XGBoost training parameters as follows: (1) *eta* = 0.05 (learning rate controller); (2) *nrounds* = 3000 (number of iterations); (3) *gamma* = 4 (the amount of loss reduction); (4) *max_depth* = 4 (the depth of training trees); (5) *min_child_weight* = 4 (conservative model determination); and (6) *alpha* = *lambda* = 4 (regularization parameters).

Third, the reconstructed GRACE/GRACE-FO product is assessed using Pearson's correlation coefficient (CC), Nash-Sutcliffe efficiency (NSE), and scaled root mean square error (RMSE*) indicators. Models with CC > 0.8, RMSE* < 0.5, and NSE > 0.7 are considered effective (Gyawali et al., 2022).

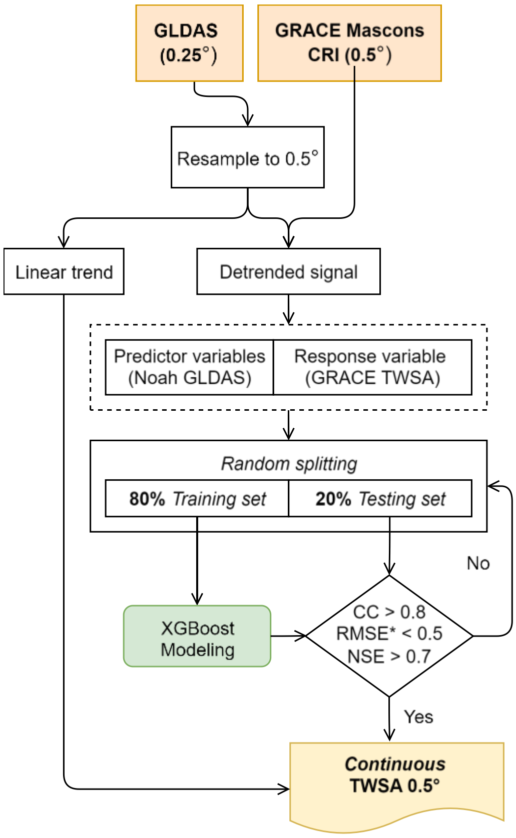

Figure 2. Research processing flowcharts.

Results and Discussion

1. Gap-filling Reconstruction and Uncertainties

In evaluating the XGBoost model, the performance metrics of CC, NSE, and RMSE* were found to be (training/testing set) 0.978/0.943, 0.954/0.887, and 0.215/0.337, respectively. The scatter plot visualization of original and predicted detrended GRACE TWSA in centimeter unit is shown in Figure 3. Furthermore, Figure 4 shows the grid-scale performance of the XGBoost model for both training and testing sets, evaluated using

CC, NSE, and RMSE* values for each pixel. In the testing set of 134 pixels across five basins, 126 pixels (94.03%) had "Very Strong" CC, 6 pixels (4.45%) "Strong," 1 pixel (0.75%) "Medium,", and 1 pixel (0.75%) showed negative CC. For NSE, 112 pixels (83.58%) were "Very Good," 14 pixels (10.45%) "Good," and 4 pixels (2.99%) "Satisfactory," with 4 pixels (2.99%) "Unsatisfactory", and two of these being negative. For RMSE*, 106 pixels (79.10%) had RMSE* ≤ 0.5, 26 pixels (19.40%) were between 0.5 and 1.0, and 2 pixels (1.49%) were ≥ 1.0.

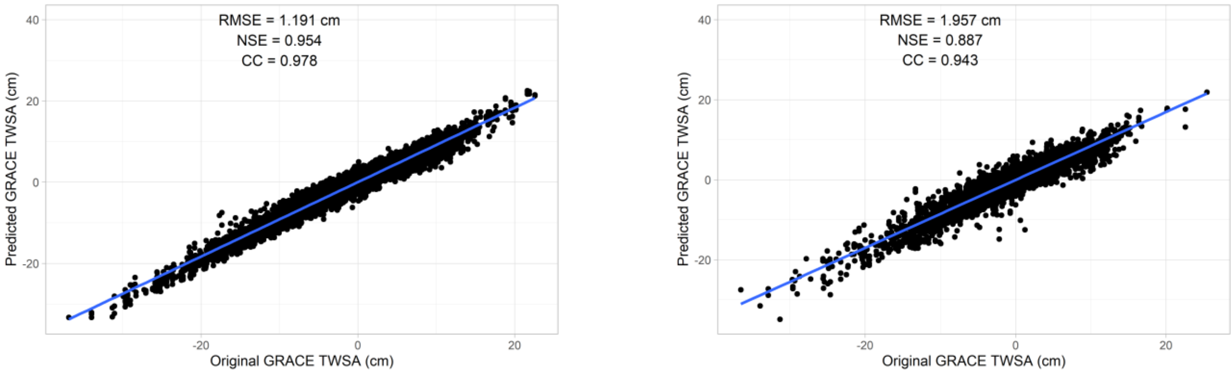

(a) (b)

Figure 3. Scatter plot of original and predicted GRACE TWSA using XGBoost model on (a) training set and (b) testing set.

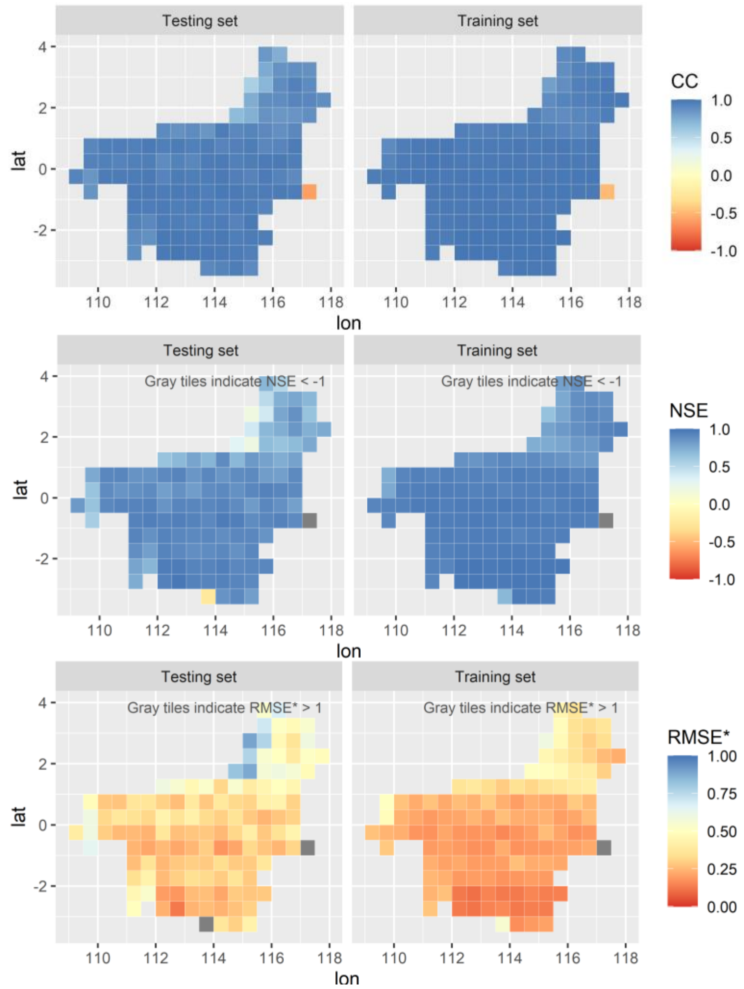

Figure 4. XGBoost model's performance at grid scale for training and testing sets.

While the XGBoost model demonstrates strong overall performance, the suboptimal results observed in specific pixels may be influenced by several factors. Firstly, leakage errors may have contributed to the unsatisfactory performance at these pixels, potentially exaggerating or reducing GRACE signal values along the coastal regions. Hydrological signals in the ocean are significantly smaller than those on land, leading to contamination between the two domains and affecting the accuracy of EWH (cm) quantification (Seo et al., 2020; Zou & Jin, 2014). Additionally, uncertainties in input data, including GRACE TWSA and Noah GLDAS predictor variables, contribute to overall uncertainty. These uncertainties fluctuate due to variations in solid earth mass, snow cover, and the number of iterations used in the model. Furthermore, non-climatic parameters not included in the modeling, such as anthropogenic activities like groundwater irrigation, could influence TWSA but are not accounted for in this study. This limitation suggests that while hydrological variables enhance prediction accuracy in specific spatial and temporal scales, they may not sufficiently explain TWSA under significant anthropogenic impacts (Li et al., 2019; Seyoum et al., 2019). Lastly, the increasing frequency of extreme hydroclimatic events, such as those driven by El Niño and La Niña within the ENSO cycle, poses additional challenges to the model's performance (Wan et al., 2023).

Building on these insights, we applied the XGBoost model with the following training parameters: (1) *eta* = 0.05, (2) *nrounds* = 3000, (3) *gamma* = 4, (4) *max_depth* = 4, (5) *min_child_weight* = 4, and (6) *alpha* = *lambda* = 4, utilizing hydrological variables as predictors to reconstruct detrended and full-signal TWSA in EWH (cm) over an 11-month gap in GRACE satellite data. The results, depicted as blue time series lines in Figure 5, represent the average pixel values across training, testing, and the gap period, providing a comprehensive monthly TWSA.

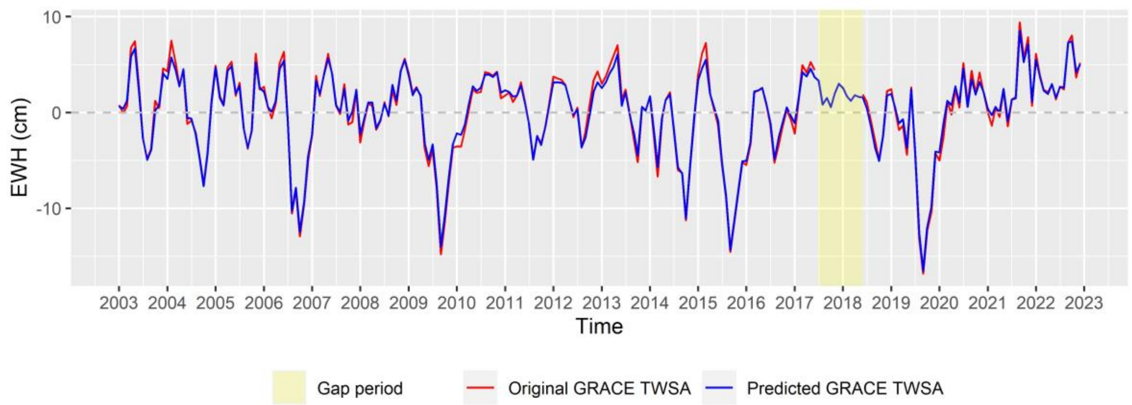

(a)

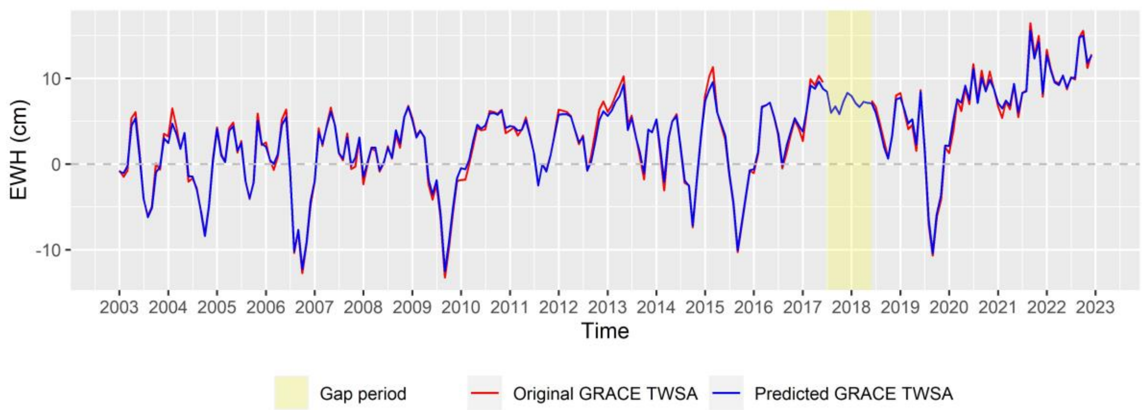

(b)

Figure 5. Signal reconstruction results: (a) detrended TWSA and (b) full TWSA signal using XGBoost model for the period of 2003-2022 over Kalimantan basins.

2. Precision Compared to Previous Studies

To evaluate the modeling precision in this study, the predicted and reconstructed detrended TWSA signals were compared with the detrended TWSA signals from previous research by Li et al. (2021), using a 0.5° resolution and the CC metric. Figure 6 presents the monthly average detrended TWSA for each basin under investigation. In the figure, the red line represents the original GRACE data, the blue line depicts the predicted TWSA from this study (referred to as $TWSA_{D_{Rec}}$), and the orange line indicates the predicted TWSA from Li et al. (2021) (referred to as $TWSA_{D_{Li}}$). Overall, including the gap months, $TWSA_{D_{Rec}}$ and $TWSA_{D_{Li}}$ exhibit similar patterns, though with different amplitude variations. Notable discrepancies in amplitude are observed in the NKB basin, where the original TWSA and $TWSA_{D_{Rec}}$ signals are underestimated from January to July 2008, July 2009 to January 2010, August 2018 to January 2019, and January to June 2020, compared to $TWSA_{D_{Li}}$. Conversely, they are overestimated from June to October 2011, July 2012 to October 2013, and June to October 2014. Additionally, the NKB basin shows slightly lower CC and NSE and higher RMSE* for the original TWSA and $TWSA_{D_{Rec}}$ compared to other basins, as shown in Figure 4.

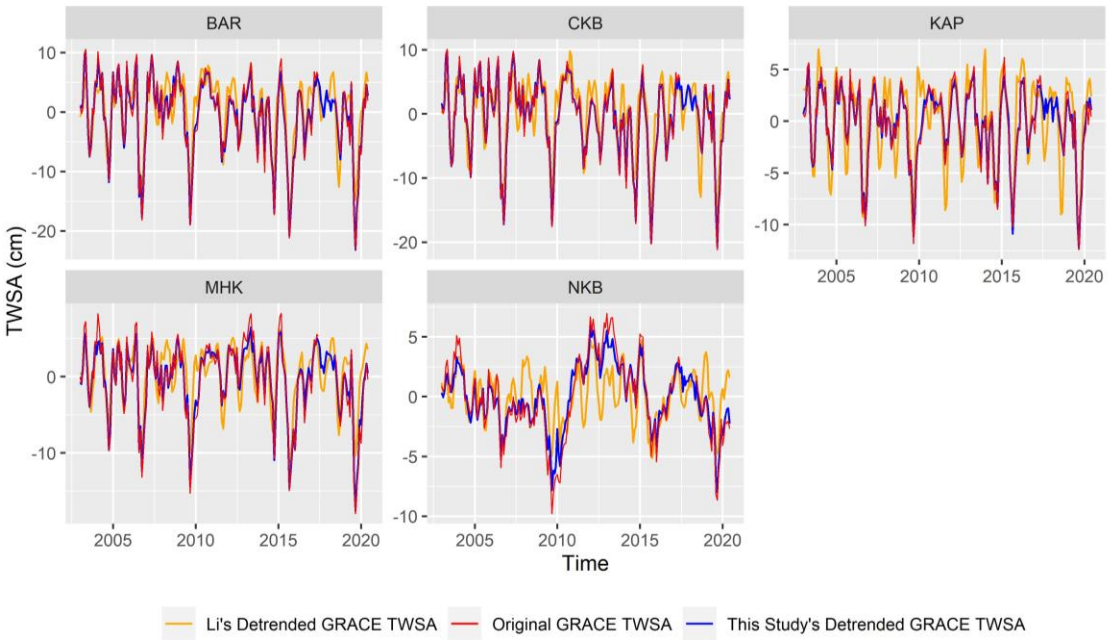

Figure 6. Time-series comparison of original GRACE TWSA (red line), this study's prediction (blue line), and Li's prediction (orange line) for the period 2003–2020 across five Kalimantan basins.

In Figure 7, the quantitative relationships between Li's and this study's GRACE TWSA predictions relative to the original GRACE TWSA Mascon CRI product are depicted. The BAR basin exhibited the highest performance, with CC, NSE, and RMSE* values of 0.854, 0.561, and 0.661, respectively, in comparison to the original GRACE TWSA. Conversely, the NKB basin displayed the lowest scores, with a CC of 0.628, NSE of -0.455, and RMSE* of 1.203. The TWSA prediction of this study demonstrated a strong correlation with the original GRACE TWSA, as indicated by the metrics computed for training and testing predictions. In this regard, CKB exhibited the highest performance, with CC, NSE, and RMSE* values of 0.997, 0.994, and 0.080, respectively. In contrast, NKB displayed slightly lower performance, with CC, NSE, and RMSE* values of 0.979, 0.884, and 0.340, respectively. Furthermore, the assessment of the relationship between Li's TWSA prediction and the outcome of this study resulted in varied metric scores, ranging from a CC of 0.639 for the NKB basin to a CC of 0.870 for the BAR basin, an NSE of 0.048 for the NKB basin to 0.635 for the BAR basin, and an RMSE* of 0.603 for BAR to 0.974 for the NKB basin.

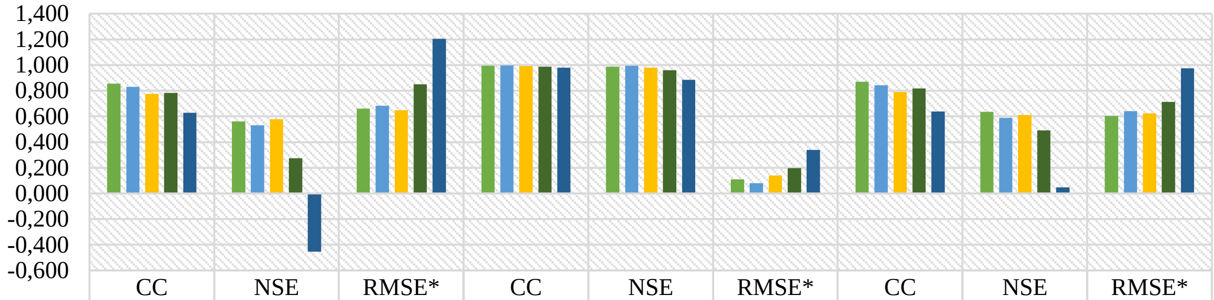

	Li's vs. Original GRACE TWSA			This Study vs. Original GRACE TWSA			Li's vs. This Study		
	CC	NSE	RMSE*	CC	NSE	RMSE*	CC	NSE	RMSE*
BAR	0,854	0,561	0,661	0,995	0,988	0,111	0,870	0,635	0,603
CKB	0,830	0,530	0,684	0,997	0,994	0,080	0,842	0,587	0,641
KAP	0,775	0,579	0,647	0,992	0,980	0,139	0,789	0,610	0,623
MHK	0,783	0,275	0,850	0,987	0,961	0,197	0,816	0,491	0,712
NKB	0,628	-0,455	1,203	0,979	0,884	0,340	0,638	0,048	0,974

Figure 7. Statistical metrics for Li's study, this study, and the original GRACE TWSA across five Kalimantan basins.

The variance in signal amplitude between Li's prediction results and the present study may arise from various factors.

(1) Variations in input data are notable, as this study utilizes GRACE Mascon input data with a CRI filter developed by JPL. Conversely, Li et al. (2021) employed the Mascon solution generated by CSR without the CRI filter (Save et al., 2016), potentially leading to distinct estimations of TWSA trends (Jing et al., 2019). Additionally, this study incorporates P, ET, Q, SMSA, PCSA, N, and T as driving factors in TWSA prediction, while Li et al. (2021) utilized T (2 m), P, sea surface temperature (SST), 17 climatological indices, SMS, Q, and ET.

(2) Differences in modeling schemes exist between the two studies. This study applies the random splitting method to segregate input data into two sets over specific periods, employing XGB and RF algorithms for training. Conversely, Li et al. (2021) splits the data differently and utilized MLR, ANN, and ARX algorithms from their own framework.

(3) Differences in research scale are evident; Li et al.'s (2020) global-scale study covers a broader and more intricate range of signals, especially in diverse climate regions, not observable at a local modeling scale (Zhou et al., 2017).

Conclusions

This research employs the Extreme Gradient Boosting (XGBoost) algorithm to reconstruct the Terrestrial Water Anomaly (TWSA) across five basins in Kalimantan using GRACE Mascon data. TWSA serves as the response variable, while the input variables comprise precipitation (P), evapotranspiration (ET), runoff (Q), soil moisture storage anomaly (SMSA), plant canopy storage anomaly (PCSA), Noah-derived TWSA (N), and temperature (T), each with a three-month time lag effect. The data, encompassing response variables and predictors, were detrended at a 0.5° resolution from 2003 to 2022, with an extended gap between July 2017 and May 2018. The data was randomly partitioned into training (80%) and testing (20%) sets. The XGBoost model, with training parameters set as follows: (1) eta = 0.05; (2) nrounds = 3000; (3) gamma = 4; (4) max_depth = 4; (5) min_child_weight = 4; and (6) alpha = lambda = 4, achieved the evaluation metrics of CC, NSE, and RMSE* on the testing set, yielding 0.943, 0.887, and 0.337, respectively. At the pixel scale, strong CC and NSE performances were observed in 94.03% and 83.58% of cases, with 79.10% of pixels exhibiting RMSE < 0.5. Validation against Li's study (2021) demonstrated a CC of 0.639 for the NKB basin and 0.870 for the BAR basin. This study recommends additional pre-processing to determine the strongest relationship between various GRACE Mascons global data products and TWS conditions in the study area. The analysis can be refined using the water budget equation, where the change in TWS equals the precipitation value minus evapotranspiration and runoff. Meteorological data from local meteorological stations should enhance the precision of adding and subtracting TWS in the study area.

Acknowledgment

The author would like to thank the Jet Propulsion Laboratory and NASA Land Data Assimilation system for providing the primary data for this research.

References

Ali, S., Khorrami, B., Jehanzaib, M., Tariq, A., Ajmal, M., Arshad, A., Shafeeque, M., Dilawar, A., Basit, I., Zhang, L., Sadri, S., Niaz, M. A., Jamil, A., & Khan, S. N. (2023). Spatial Downscaling of GRACE Data Based on XGBoost Model for Improved Understanding of Hydrological Droughts in the Indus Basin Irrigation System (IBIS). *Remote Sensing*, *15*(4), 873. https://doi.org/10.3390/rs15040873

Ali, S., Liu, D., Fu, Q., Cheema, M. J. M., Pal, S. C., Arshad, A., Pham, Q. B., & Zhang, L. (2022). Constructing high-resolution groundwater drought at spatio-temporal scale using GRACE satellite data based on machine learning in the Indus Basin. *Journal of Hydrology*, *612*(PC), 128295. https://doi.org/10.1016/j.jhydrol.2022.128295

Alshehri, F., & Mohamed, A. (2023). Analysis of Groundwater Storage Fluctuations Using GRACE and Remote Sensing Data in Wadi As-Sirhan, Northern Saudi Arabia. *Water (Switzerland)*, *15*(2). https://doi.org/10.3390/w15020282

Awange, J. L., Sharifi, M. A., Ogonda, G., Wickert, J., Grafarend, E. W., & Omulo, M. A. (2008). The Falling Lake Victoria Water Level: GRACE, TRIMM and CHAMP Satellite Analysis of the Lake Basin. *Water Resources Management*, *22*(7), 775–796. https://doi.org/10.1007/s11269-007-9191-y

Barker, L. J., Hannaford, J., Chiverton, A., & Svensson, C. (2016). From meteorological to hydrological drought using standardised indicators. *Hydrology and Earth System Sciences*, *20*(6), 2483–2505. https://doi.org/10.5194/hess-20-2483-2016

Beaudoing, H., & Rodell, M. (2020). *GLDAS Noah Land Surface Model L4 monthly 0.25 x 0.25 degree V2.1*. Goddard Earth Sciences Data and Information Services Center (GES DISC). https://doi.org/10.5067/SXAVCZFAQLNO

BMKG. (2021). *Climate Change Assessment in Indonesia*. https://iklim.bmkg.go.id/publikasi-klimat/ftp/brosur/LEAFLETINGGRISB.pdf

Chen, T., & Guestrin, C. (2016). XGBoost: A scalable tree boosting system. *Proceedings of the ACM SIGKDD International Conference on Knowledge Discovery and Data Mining*, *13-17-Augu*, 785–794. https://doi.org/10.1145/2939672.2939785

Chen, T., He, T., Benesty, M., & Khotilovich, V. (2020). *Package 'xgboost.'* R Version 2020, Volume 90. https://cran.r-project.org/web/packages/xgboost/index.html

Cui, A. (2019). Hydrological drought measurement using GRACE terrestrial water storage anomaly. In *International Geoscience and Remote Sensing Symposium (IGARSS)* (pp. 9914–9917). https://doi.org/10.1109/IGARSS.2019.8898939

Girotto, M., & Rodell, M. (2019). Terrestrial water storage. In *Extreme Hydroclimatic Events and Multivariate Hazards in a Changing Environment: A Remote Sensing Approach*. Elsevier Inc. https://doi.org/10.1016/B978-0-12-814899-0.00002-X

Gyawali, B., Ahmed, M., Murgulet, D., & Wiese, D. N. (2022). Filling Temporal Gaps within and between GRACE and GRACE-FO Terrestrial Water Storage Records: An Innovative Approach. *Remote Sensing*, *14*(7), 1565. https://doi.org/10.3390/rs14071565

Humphrey, V., Rodell, M., & Eicker, A. (2023). Using Satellite-Based Terrestrial Water Storage Data: A Review. *Surveys in Geophysics*, *44*(5), 1489–1517. https://doi.org/10.1007/s10712-022-09754-9

Jiang, W., Ji, X., Li, Y., Luo, X., Yang, L., Ming, W., Liu, C., Yan, S., Yang, C., & Sun, C. (2023). Modified flood potential index (MFPI) for flood monitoring in terrestrial water storage depletion basin using GRACE estimates. *Journal of Hydrology*, *616*, 128765. https://doi.org/10.1016/j.jhydrol.2022.128765

Jing, W., Zhang, P., & Zhao, X. (2019). A comparison of different GRACE solutions in terrestrial water storage trend estimation over Tibetan Plateau. *Scientific Reports*, *9*(1), 1765. https://doi.org/10.1038/s41598-018-38337-1

Kumar, K. S., Sridhar, V., Varaprasad, B. J. S., & Chinnapa Reddy, K. (2022). Bridging the Data Gap between the GRACE Missions and Assessment of Groundwater Storage Variations for Telangana State, India. *Water*, *14*(23), 3852. https://doi.org/10.3390/w14233852

Lai, Y., Zhang, B., Yao, Y., Liu, L., Yan, X., He, Y., & Ou, S. (2022). Reconstructing the data gap between GRACE and GRACE follow-on at the basin scale using artificial neural network. *Science of The Total Environment*, *823*,

153770. https://doi.org/10.1016/j.scitotenv.2022.153770
Li, F., Kusche, J., Chao, N., Wang, Z., & Löcher, A. (2021). Long-Term (1979-Present) Total Water Storage Anomalies Over the Global Land Derived by Reconstructing GRACE Data. *Geophysical Research Letters*, *48*(8). https://doi.org/10.1029/2021GL093492
Li, Wang, Zhang, Wen, Zhong, Zhu, & Li. (2019). Bridging Terrestrial Water Storage Anomaly During GRACE/GRACE-FO Gap Using SSA Method: A Case Study in China. *Sensors*, *19*(19), 4144. https://doi.org/10.3390/s19194144
Mediawan, Y., Montarcih, L., Soetopoi, W., & Prayogo, T. B. (2021). Water Balance Supporting the Irrigation Water Demand in Java Island, Indonesia. *Indonesian Journal of Geography*, *53*(1), 9–19. https://doi.org/10.22146/ijg.59102
Melo, D. de C. D., & Wendland, E. (2016). Hydrological system time lag responses to meteorological shifts. *RBRH*, *21*(4), 766–776. https://doi.org/10.1590/2318-0331.011616083
Mo, S., Zhong, Y., Forootan, E., Mehrnegar, N., Yin, X., Wu, J., Feng, W., & Shi, X. (2022). Bayesian convolutional neural networks for predicting the terrestrial water storage anomalies during GRACE and GRACE-FO gap. *Journal of Hydrology*, *604*, 127244. https://doi.org/10.1016/j.jhydrol.2021.127244
Pusat Data dan Sistem Informasi Pertanian. (2020). *Statistik Lahan Pertanian Tahun 2015-2019*. https://satudata.pertanian.go.id/assets/docs/publikasi/Statistik_Lahan_Pertanian_Tahun_2015-2019.pdf
Rateb, A., Save, H., Sun, A. Y., & Scanlon, B. R. (2024). Rapid mapping of global flood precursors and impacts using novel five-day GRACE solutions. *Scientific Reports*, *14*(1), 13841. https://doi.org/10.1038/s41598-024-64491-w
Sahour, H., Sultan, M., Vazifedan, M., Abdelmohsen, K., Karki, S., Yellich, J. A., Gebremichael, E., Alshehri, F., & Elbayoumi, T. M. (2020). Statistical applications to downscale GRACE-derived terrestrialwater storage data and to fill temporal gaps. *Remote Sensing*, *12*(3). https://doi.org/10.3390/rs12030533
Save, H., Bettadpur, S., & Tapley, B. D. (2016). High-resolution CSR GRACE RL05 mascons. *Journal of Geophysical Research: Solid Earth*, *121*(10), 7547–7569. https://doi.org/10.1002/2016JB013007
Senent-Aparicio, J., Liu, S., Pérez-Sánchez, J., López-Ballesteros, A., & Jimeno-Sáez, P. (2018). Assessing Impacts of Climate Variability and Reforestation Activities on Water Resources in the Headwaters of the Segura River Basin (SE Spain). *Sustainability*, *10*(9), 3277. https://doi.org/10.3390/su10093277
Seo, K.-W., Oh, S., Eom, J., Chen, J., & Wilson, C. R. (2020). Constrained Linear Deconvolution of GRACE Anomalies to Correct Spatial Leakage. *Remote Sensing*, *12*(11), 1798. https://doi.org/10.3390/rs12111798
Seyoum, W., Kwon, D., & Milewski, A. (2019). Downscaling GRACE TWSA Data into High-Resolution Groundwater Level Anomaly Using Machine Learning-Based Models in a Glacial Aquifer System. *Remote Sensing*, *11*(7), 824. https://doi.org/10.3390/rs11070824
Sun, Z., Long, D., Yang, W., Li, X., & Pan, Y. (2020). Reconstruction of GRACE Data on Changes in Total Water Storage Over the Global Land Surface and 60 Basins. *Water Resources Research*, *56*(4), 1–21. https://doi.org/10.1029/2019WR026250
Tapley, B. D., Watkins, M. M., Flechtner, F., Reigber, C., Bettadpur, S., Rodell, M., Sasgen, I., Famiglietti, J. S., Landerer, F. W., Chambers, D. P., Reager, J. T., Gardner, A. S., Save, H., Ivins, E. R., Swenson, S. C., Boening, C., Dahle, C., Wiese, D. N., Dobslaw, H., … Velicogna, I. (2019). Contributions of GRACE to understanding climate change. *Nature Climate Change*, *9*(5), 358–369. https://doi.org/10.1038/s41558-019-0456-2
Tirtalistyani, R., Murtiningrum, M., & Kanwar, R. S. (2022). Indonesia Rice Irrigation System: Time for Innovation. *Sustainability*, *14*(19), 12477. https://doi.org/10.3390/su141912477
Wan, X., You, W., Kusche, J., Li, F., Yang, X., Fan, D., Pu, L., & Jiang, Z. (2023). Evaluating different predictive strategies for filling the global GRACE/-FO terrestrial water storage anomalies gap. *Journal of Hydrology*, *626*(PA), 130216. https://doi.org/10.1016/j.jhydrol.2023.130216
Wang, J., Chen, Y., Wang, Z., & Shang, P. (2020). Drought evaluation over Yangtze River basin based on weighted water storage deficit. *Journal of Hydrology*, *591*(July), 125283. https://doi.org/10.1016/j.jhydrol.2020.125283
Wang, J., Shen, Y., Awange, J. L., & Yang, L. (2023). A deep learning model for reconstructing centenary water storage changes in the Yangtze River Basin. *Science of The Total Environment*, *905*(September), 167030. https://doi.org/10.1016/j.scitotenv.2023.167030
Wiese, D. N., Yuan, D.-N., Boening, C., Landerer, F. W., & Watkins, M. M. (2023). *JPL GRACE and GRACE-FO Mascon Ocean, Ice, and Hydrology Equivalent Water Height CRI Filtered. Ver. RL06.1Mv03*. TELLUS. https://doi.org/10.5067/TEMSC-3JC63
Wurbs, R. A. (2005). Modeling river/reservoir system management, water allocation, and supply reliability. *Journal of Hydrology*, *300*(1–4), 100–113. https://doi.org/10.1016/j.jhydrol.2004.06.003
Xiong, J., Yin, J., Guo, S., & Slater, L. (2021). Continuity of terrestrial water storage variability and trends across mainland China monitored by the GRACE and GRACE-Follow on satellites. *Journal of Hydrology*, *599*(March), 126308. https://doi.org/10.1016/j.jhydrol.2021.126308
Yang, P. (2017). Monitoring the spatio-temporal changes of terrestrial water storage using GRACE data in the Tarim

River basin between 2002 and 2015. *Science of the Total Environment*, *595*, 218–228. https://doi.org/10.1016/j.scitotenv.2017.03.268

Zhang, J., Liu, K., & Wang, M. (2021). Downscaling groundwater storage data in China to a 1-km resolution using machine learning methods. *Remote Sensing*, *13*(3), 1–19. https://doi.org/10.3390/rs13030523

Zhou, H., Luo, Z., Tangdamrongsub, N., Wang, L., He, L., Xu, C., & Li, Q. (2017). Characterizing Drought and Flood Events over the Yangtze River Basin Using the HUST-Grace2016 Solution and Ancillary Data. *Remote Sensing*, *9*(11), 1100. https://doi.org/10.3390/rs9111100

Zhu, E., Wang, Y., & Yuan, X. (2023). Changes of terrestrial water storage during 1981–2020 over China based on dynamic-machine learning model. *Journal of Hydrology*, *621*(April). https://doi.org/10.1016/j.jhydrol.2023.129576

Zou, F., & Jin, S. (2014). Land-ocean leakage errors in satellite gravity measurements using forward modeling. *2014 Third International Workshop on Earth Observation and Remote Sensing Applications (EORSA)*, 19–23. https://doi.org/10.1109/EORSA.2014.6927841